

Identifying Best Candidates for Busbar Splitting

Giacomo Bastianel, Dirk Van Hertem, Hakan Ergun KU Leuven / Etch - EnergyVille
Leuven / Genk, Belgium

{giacomo.bastianel, dirk.vanhertem, hakan.ergun}@kuleuven.be

Line A. Roald

University of Wisconsin - Madison,
Madison, WI, USA
roald@wisc.edu

Abstract—Rising electricity demand and the growing integration of renewables are intensifying congestion in transmission grids. Grid topology optimization through busbar splitting (BuS) and optimal transmission switching can alleviate grid congestion and reduce the generation costs in a power system. However, BuS optimization requires a large number of binary variables, and analyzing all the substations for potential new topological actions is computationally intractable, particularly in large grids. To tackle this issue, we propose a set of metrics to identify and rank promising candidates for BuS, focusing on finding buses where topology optimization can reduce generation costs. To assess the effect of BuS on the identified buses, we use a combined mixed-integer convex-quadratic BuS model to compute the optimal topology and test it with the non-linear non-convex AC optimal power flow (OPF) simulation to show its AC feasibility and generation cost reduction compared to the AC-OPF simulations. By testing and validating the proposed metrics on test cases of different sizes, we show that they are able to identify busbars that reduce the total generation costs when their topology is optimized. Thus, the metrics enable effective selection of busbars for BuS, with no need to test every busbar in the grid, one at a time.

Index Terms—Busbar Splitting, Grid-Enhancing Technologies, Grid Topology Optimization, Metrics, Topological Actions, Remedial Actions, Transmission Grids.

I. Introduction and motivation

With the increasing urgency to decrease global CO₂ emissions, societies are becoming increasingly electrified. As a result, electricity demand is projected to increase significantly [1]. However, due to the limited transmission capacity and the distributed nature of newly-installed renewable energy sources (RES) capacity [2], power systems worldwide are facing increasing congestion [1]. In both Europe [3] and the US [4,5], congestion costs have seen a substantial increase in recent years, reaching e.g. 2.774 bn€ in 2024 in Germany [6], and 13.5-8.33 bn\$ in 2023 and 2024 for all the US Independent System Operators [4,5]. Currently, power grids are considered an important bottleneck for a carbon-free society, and the deployment of RES requires additional transmission capacity [1]. Significant RES curtailment will take place without effective grid expansion projects aimed to increase the grid transmission capacity [7]. At the same time, expanding the grid requires worldwide investments in the range of hundreds of billions €/ \$ per year [8]. Besides economic reasons, grid expansion projects are

often delayed due to technical (supply chain issues, lack of workforce, lack of manufacturing capacity, bottlenecks with critical elements, etc. [9]) and non-technical (public opposition [10]) issues. Because of all these reasons, system operators are currently aiming to maximize the transmission capacity in the existing grid to reduce existing congestion. For example, congestion management actions such as power flow control can be performed, among the others, with phase-shifting transformers and high-voltage direct current links. A broader term to describe these technologies is “grid-enhancing technologies” [11], which also includes flexible AC transmission technologies and dynamic line rating. Although the attention surrounding these technologies is increasing [12], in Europe, they are still primarily applied to maximize cross-border flows, while additional costly remedial measures are employed to address internal grid congestion.

Consequently, several initiatives in Europe [13] and the US [12,14] aim to improve the utilization of existing grid infrastructure by actively optimizing and reconfiguring the network topology to mitigate congestion and maximize transfer capacity. However, the available topological actions, such as OTS and substation reconfiguration with BuS are often restricted to well-established, expert-driven measures that system operators have employed for decades, even though the power flows through transmission grids are rapidly changing. As a result, potentially effective topological actions remain unidentified, and systematic methodologies to discover them are yet to be established in the scientific literature. In particular, while the most common topological actions in industry include substation reconfiguration through BuS, academic papers investigating topology optimization with BuS are relatively new, in part because BuS is computationally highly challenging. Every busbar considered in the topology optimization problem introduces a new degree of freedom and thus has the potential to reduce generation costs compared to a standard OPF by solving congestion, therefore allowing the cheaper generators to be used to their maximum rated power, but representing multiple possible splitting configurations requires the use of binary variables and thus adds significant computational complexity. When implementing topology optimization for larger grids, it is therefore necessary to pre-screen

busbars to identify promising candidate busbars for BuS. This paper addresses this issue by proposing metrics to identify efficient topological actions in transmission grids based on the results of optimal power flow (OPF) simulations. Although several metrics (discussed later) have been proposed in the literature, no prior work has systematically assessed their effectiveness in identifying the most suitable busbars for applying topological actions through BuS. In a rapidly evolving power system, such metrics can support system operators in identifying new impactful topological actions, ultimately maximizing the grid’s power transfer capacity.

A. Related work and contributions

The concept of topology optimization using optimal transmission switching (OTS) and busbar splitting (BuS) has been utilized for decades to manage contingencies [15], reduce the total generation costs (OTS [16,17] and BuS [18]), relieve grid congestion, and plan maintenance. While the first ideas to filter and select the most relevant network elements to be switched were developed decades ago for [19,20], and there is a considerable body of literature on OTS [21], its extensions [22] and application related to contingency analysis [17], the proposal to use BuS to optimize the substation configuration and achieve reductions in the total generation costs is fairly recent [23]–[26] and has been applied to hybrid AC/DC grids, too [27]–[30].

Most literature is based on the concept of locational marginal price (LMP), defined as “the marginal cost of delivering one more unit of electricity to a specific bus, taking into account transmission losses and network constraints” [31]. LMPs depend on the location where electricity is generated or consumed, and are usually higher in areas that normally import power and lower in areas that export power [32]. From a mathematical perspective, LMPs can be derived as the Lagrange multiplier associated with the nodal balance constraint in the OPF formulation [32].

References [33] and [34] propose a heuristic to select the most relevant lines to be switched in the OTS problem based on the difference in LMPs between the two ends of a branch, multiplied by the power flow through the branch. Additional sensitivity criteria for line selection are investigated in [35]. Moreover, potential remedial actions are identified by studying congestion zones in [36] for the OTS problem and in [23,37] for the BuS problem. [25] extends the methodology in [23] by adding a pre-screening step that uses LMPs associated with active and reactive power and only considers substations with four or more connected lines to identify relevant busbars for OTS. Other references [38,39] develop heuristics for selecting the most relevant busbars in BuS based on the load margin [38] and for selecting the best breakers in node-breaker modelling [39] using i) the maximum increase in the congestion rent, ii) the reduction in total generation costs and iii) the largest absolute value of LMP difference across

TABLE I
Overview of common metrics in the literature related to optimal transmission switching (OTS) and busbar splitting (BuS). “LMP” stands for “locational marginal price”. “ Δ_{LMP} ” stands for the difference in LMPs over a branch.

Identified metric	OTS-Related	BuS-Related
$(\Delta_{LMP}) \cdot$ (branch power flow)	[33,34]	-
Congested lines/zones identification	[36]	[23,25,37]
Load margin	-	[38]
Increase in congestion rent	[39]	-
Δ_{LMP}	-	[25,39]
# of elements connected to the busbar	-	[25,26]

any line in the system. The latter metric is similar to [33], but without considering the power through the lines. Finally, [26] selects buses with ten or more connected components as candidates for topology optimization. The existing above-mentioned metrics to select the most relevant elements for grid topology optimization mainly rely on single Δ_{LMP} s through a branch connected to a given busbar, without including Δ_{LMP} patterns throughout all the branches connected to it. In addition, except for [25], they rely on the linear DC approximation of the OPF problem, without considering the grid’s reactive power and voltage magnitude levels. These factors are becoming increasingly important in modern converter-dominated power systems, and their mismanagement could lead to events such as the Iberian blackout in April 2025 [40].

In previous work [27,29], we observed that only certain busbars lead to a reduction in generation costs when only one busbar was allowed to be split at a time. However, if applied to a large system, having to exhaustively check all busbars adds a significant computational cost to the optimization problem. The goal in this paper is therefore to identify a small subset of busbars that will reduce generation cost if we optimize their topology. These busbars are selected a priori through the proposed metrics, based on the grid topology and on the results of the AC-OPF formulation.

Table I summarizes the most relevant metrics emerging from the literature, and whether they were related to OTS or BuS in the aforementioned publications. The new metrics proposed in this work are introduced later in Section III.

B. Contributions

This paper improves on the state of the art in the field of steady-state grid topology optimization by:

- Identifying and validating metrics to select relevant busbar candidates to perform busbar splitting on AC grids ranging from 39 to thousands of buses, with the final objective of reducing the total generation costs. The pre-emptive selection of relevant candidates for busbar splitting identifies zones where grid topology optimization is relevant without the need to investigate the whole grid.
- Validating the topology optimized with the busbar splitting model introduced in [27,29], based on a

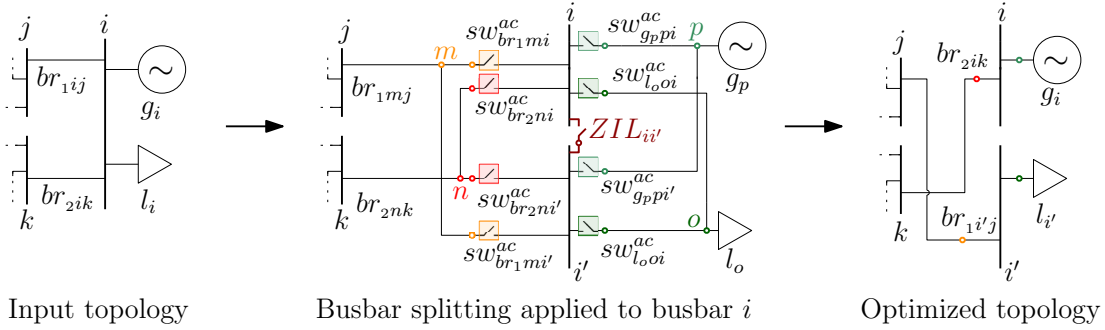


Fig. 1. Steps behind the topology optimization model proposed in [27,29]. The selected busbar i (left) is split into two buses i and i' , connected through a busbar coupler $ZIL_{ii'}$. The open/close position of this busbar coupler $ZIL_{ii'}$ is represented in the optimization model by a binary variable. Each network element that was connected to busbar i in the input topology is linked to an auxiliary bus (named m, n, o and p in the figure) and can be connected to either one (i) or the other part (i') of the split busbar through a switch (center). Each switch is also represented in the model through a binary variable. After the optimization, the inactive switches are removed to yield the new topology (right).

piecewise linear approximation (LPAC) of the AC-optimal power flow (OPF) formulation, with respect to LPAC- and AC-OPF simulations, obtaining feasible and optimal results.

The remainder of this work is organized as follows. Section II describes the existing topology optimization model used in the paper, while Section III describes the proposed metrics for selecting the best candidates for busbar splitting. Section IV discusses the results, with Section V concluding the paper, and highlighting possible avenues for future work.

II. Preliminaries: Topology Optimization with Busbar Splitting

This paper is based on the grid topology optimization model introduced in [27,29], which includes BuS of selected busbars based on an LPAC-OPF formulation. This model gives rise to a mixed-integer, convex-quadratic optimization problem that can be solved efficiently compared with a formulation that uses the full non-convex, non-linear AC power flow constraints, while also providing results that are typically AC-feasible [27,29].

Once we obtain the optimized topology, we evaluate the cost reduction by solving the AC-OPF from [41] with the original and optimized topologies. For brevity, we refer the reader to [41] for a thorough explanation of the detailed LPAC- and AC-OPF formulations, while here we add the LPAC-BuS model from [27], and we focus on explaining the logical constraints used to represent the BuS actions in the model to highlight their inherent complexity.

A. Intuition behind busbar splitting

Fig. 1 provides an example of a busbar with two branches, a generator and a load. To represent BuS actions for busbar i in Fig. 1 (left), we remove all grid elements connected to the busbar and instead connect them to new auxiliary busbars. Then, the original bus is split into two buses i and i' . For each component, we introduce a pair of switches sw_{vmi}^{ac} and $sw_{\kappa mi'}^{ac}$ to represent which part of the

split busbar the component can be connected to. Each component cannot be connected to more than one bus, but can be completely disconnected. We also introduce a binary variable $sw_{ZIL_{ii'}}^{ac}$ to represent the open/close status of the busbar coupler, which connects the busbars i and i' . If the busbar coupler $sw_{ZIL_{ii'}}^{ac}$ is closed, the two parts of the AC busbar are connected, and AC buses i and i' have the same voltage angle and magnitude values. This reasoning is translated into the optimization model from [27,29] in the following Section.

B. Grid topology optimization model

The nomenclature of the network components, topologies and connectivities used throughout the Section are included in Table II. Note that by using ‘reverse’ topologies for the branches, power flows in both directions can be represented in the OPF and BuS models [41].

The LPAC-BuS model is represented by the equations (M1.1)-(M1.18), as shown in Model 1. The objective function in (M1.1) consists of i) minimizing the total costs of the \mathcal{G} set of generators, where P_k^g is the active power injection, and ii) adding a (small) penalty term c_{ZIL} to the busbar couplers \mathcal{C} to split a busbar only if it actually brings economic benefit. All the generators k in the network are assigned cost parameters c_{2k} ($\$/W^2$), c_{1k} ($\$/W$), c_{0k} ($\$$). Note that the quadratic cost term of each generator is assigned to zero.

Eq. (M1.2) sets the voltage angle of the reference bus to zero while (M1.3) and (M1.4) limit respectively the voltage magnitude and angles of the other buses between minimum ($\underline{U}_i^m, \underline{\theta}_i$) and maximum ($\overline{U}_i^m, \overline{\theta}_i$) values. Similarly, the generator setpoints are bounded by \underline{S}_k^g and \overline{S}_k^g in (M1.6). The power balance for each node (or substation) is included in (M1.5), with S_l^m being the nodal demand. The term $Y_i^s \cdot (1 + 2\phi_i)$ refers to the power absorbed by shunt elements connected to the node i , which are considered negligible in this paper. ϕ_i indicates the voltage magnitude change in the LPAC formulation [42]. The active and reactive power flow through the branches are modeled through (M1.7) and (M1.8), with each branch being

TABLE II

Network components, topologies and connectivities and nomenclature of each network component included in the optimization model. “BuS” stands for “busbar splitting”.

Network components	
\mathcal{I}	Set of nodes
\mathcal{L}	Set of branches
\mathcal{C}	Set of busbar couplers
\mathcal{G}	Set of generators
\mathcal{M}	Set of loads
\mathcal{I}'	Set of auxiliary nodes for BuS
\mathcal{S}	Set of auxiliary switches for BuS
Topologies and connectivities	
\mathcal{T}^{ac}	Branch topologies
$\mathcal{T}^{ac,rev}$	Reverse branch topologies
$\mathcal{T}^{sw,ac}$	Switch topologies
$\mathcal{T}^{ZIL,ac}$	Busbar coupler topologies
\mathcal{T}^{load}	Load connectivity
\mathcal{T}^{gen}	Generator connectivity
Nomenclature of each network component	
$lij \in \mathcal{T}^{ac} \subseteq \mathcal{L} \times \mathcal{I} \times \mathcal{I}$	Branches
$vii' \in \mathcal{T}^{ZIL,ac} \subseteq \mathcal{C} \times \mathcal{I} \times \mathcal{I}'$	Busbar couplers
$vmi \in \mathcal{T}^{sw,ac} \subseteq \mathcal{S} \times \mathcal{I} \times \mathcal{I}'$	Auxiliary switches for BuS
$lji \in \mathcal{T}^{ac,rev} \subseteq \mathcal{L} \times \mathcal{I} \times \mathcal{I}$	Reverse Branches
$mi \in \mathcal{T}^{load}$	Loads
$gi \in \mathcal{T}^{gen}$	Generators

represented by a π -section model [41]. These active and reactive powers are constrained by (M1.9) and (M1.10), while the piecewise linear approximation of the cosine term cs of $\cos(\theta_n - \theta_m)$ for the LPAC formulation [42] is expressed in (M1.11).

Moreover, the reasoning about BuS introduced in the previous Section is formulated through constraints (M1.12) to (M1.18) and applied to a set of switches $\mathcal{T}^{sw,ac}$ and busbar couplers $\mathcal{T}^{ZIL,ac}$, with each switching element represented by a binary variable. (M1.13) and (M1.14) are related to the voltage angles and magnitudes of the two buses at the extremes of each (sw_{vmi}^{ac}) switching element, with M_θ, M_m being big-enough M values ($2\pi, 1$). (M1.15) and (M1.16) limit the active and reactive powers of all switching elements to its maximum $\bar{P}_{vmi}^{sw,ac}, \bar{Q}_{vmi}^{sw,ac}$ and minimum values $\underline{P}_{vmi}^{sw,ac}, \underline{Q}_{vmi}^{sw,ac}$. (M1.7) and (M1.8) are “exclusivity” constraints. Line switching is allowed to be performed by modeling (M1.7) as an inequality (≤ 1) constraint. As a result, switches $z_{vmi}^{sw,ac}$ and $z_{\kappa mi'}^{sw,ac}$, connecting each network element to the parts of the split busbar, are allowed to be open simultaneously, therefore removing the network element from the split busbar. Note that (M1.7) imposes that if the busbar coupler is closed, the switch $sw_{\kappa mi',t}^{ac}$ connecting the element to the original busbar is always closed.

Model 1: Grid topology optimization model, LPAC formulation

Minimize:

$$\sum_{k \in \mathcal{G}} c_{2k} \cdot S_k^{g2} + c_{1k} \cdot S_k^g + c_{0k} + \sum_{ZILii' \in \mathcal{T}^{ZIL,ac}} c_{ZIL} \cdot z_{ZILii'}^{sw,ac} \quad (M1.1)$$

Subject to:

AC bus:

$$\theta_r = 0 \quad (M1.2)$$

$$(\underline{U}_i^m - 1) \leq \phi_i \leq (\bar{U}_i^m - 1) \quad \forall i \in \mathcal{I}, \quad (M1.3)$$

$$\underline{\theta}_i \leq \theta_i \leq \bar{\theta}_i \quad \forall i \in \mathcal{I}, \quad (M1.4)$$

$$\sum_{k \in \mathcal{G}_i} S_k^g + \sum_{l \in \mathcal{M}_i} S_l^m - Y_i^s(1 + 2\phi_i) + \sum_{vmi \in (\mathcal{T}_i^{sw,ac} \cup \mathcal{T}_i^{ZIL,ac})} S_{vmi}^{sw,ac} = \sum_{lij \in \mathcal{T}^{ac}} S_{lij}^{ac} \quad \forall i \in \mathcal{I}, \quad (M1.5)$$

Generator

$$\underline{S}_k^g \leq S_k^g \leq \bar{S}_k^g, \quad \forall k \in \mathcal{G} \quad (M1.6)$$

Branches

$$P_{lij} = (g_{s,ij} + g_{ij})(1 + 2 \cdot \phi_i) - g_{ij}(cs_{ij,wt} + \phi_i + \phi_j) - b_{ij}(\theta_i - \theta_j) \quad \forall lij \in \mathcal{T}^{ac} \cup \mathcal{T}^{ac,rev} \quad (M1.7)$$

$$Q_{lij} = (b_{s,ij} + b_{ij})(1 + 2 \cdot \phi_i) - b_{ij}(cs_{ij,wt} + \phi_i + \phi_j) - g_{ij}(\theta_i - \theta_j) \quad \forall lij \in \mathcal{T}^{ac} \cup \mathcal{T}^{ac,rev} \quad (M1.8)$$

$$|P_{lij}| \leq \bar{P}_{lij} \quad \forall lij \in \mathcal{T}^{ac} \cup \mathcal{T}^{ac,rev} \quad (M1.9)$$

$$|Q_{lij}| \leq \bar{Q}_{lij} \quad \forall lij \in \mathcal{T}^{ac} \cup \mathcal{T}^{ac,rev} \quad (M1.10)$$

$$cs_{ij,wt} \leq 1 - \frac{(1 - \cos(\Delta\theta_{ij}))}{(\Delta\theta_{ij})^2} (\theta_i - \theta_j)^2 \quad \forall lij \in \mathcal{T}^{ac} \cup \mathcal{T}^{ac,rev} \quad (M1.11)$$

Busbar Splitting

$$-(1 - z_{vmi}^{sw,ac}) \cdot M_\theta \leq \theta_m - \theta_i \leq (1 - z_{vmi}^{sw,ac}) \cdot M_\theta, \quad \forall vmi \in \mathcal{T}^{sw,ac} \cup \mathcal{T}^{ZIL,ac} \quad (M1.12)$$

$$-(1 - z_{vmi}^{sw,ac}) \cdot M_m \leq \phi_m - \phi_i \leq (1 - z_{vmi}^{sw,ac}) \cdot M_m, \quad \forall vmi \in \mathcal{T}^{sw,ac} \cup \mathcal{T}^{ZIL,ac} \quad (M1.13)$$

$$z_{vmi}^{sw,ac} \cdot \underline{P}_{vmi}^{sw,ac} \leq P_{vmi}^{sw,ac} \leq z_{vmi}^{sw,ac} \cdot \bar{P}_{vmi}^{sw,ac}, \quad \forall vmi \in \mathcal{T}^{sw,ac} \cup \mathcal{T}^{ZIL,ac} \quad (M1.14)$$

$$z_{vmi}^{sw,ac} \cdot \underline{Q}_{vmi}^{sw,ac} \leq Q_{vmi}^{sw,ac} \leq z_{vmi}^{sw,ac} \cdot \bar{Q}_{vmi}^{sw,ac}, \quad \forall vmi \in \mathcal{T}^{sw,ac} \cup \mathcal{T}^{ZIL,ac} \quad (M1.15)$$

$$(P_{vmi}^{sw,ac})^2 + (Q_{vmi}^{sw,ac})^2 \leq z_{vmi}^{sw,ac} \cdot (\bar{S}_{vmi}^{sw,ac})^2, \quad \forall vmi \in \mathcal{T}^{sw,ac} \cup \mathcal{T}^{ZIL,ac}, \quad (M1.16)$$

$$z_{vmi}^{sw,ac} + z_{\kappa mi'}^{sw,ac} \leq 1, \quad \forall (vmi, \kappa mi') \in \mathcal{T}^{sw,ac} \quad (M1.17)$$

$$z_{\kappa mi'}^{sw,ac} \leq (1 - z_{ZILii'}^{sw,ac}), \quad \forall (\kappa mi', ZILii') \in \mathcal{T}^{sw,ac} \cup \mathcal{T}^{ZIL,ac} \quad (M1.18)$$

III. Proposed Metrics to Select Candidate Busbars for Busbar Splitting

We propose a set of metrics to identify busbars that are likely to lead to cost reductions if their topology is optimized. The goal of the metrics is to avoid an exhaustive search across all buses in the network, as this might lead to prohibitive computational cost. Note that we will still consider cost reductions achieved by splitting a single busbar, as this allows us to test and validate our metrics. We leave BuS optimization with multiple busbars for future work, as this leads to a combinatorial explosion in the possible busbar selections.

A. Metric design

When designing these metrics, we only use information that can be obtained with comparatively low computational effort, such as from direct analysis of the system topology, e.g., identifying the number of network elements connected to a busbar, or from solving an AC-OPF. We further take inspiration from the metrics previously discussed in Table I to identify candidate lines to be switched in OTS problems and busbars for splitting in BuS problems. Specifically, we consider the general idea of identifying buses that are associated with congestion, have large differences in LMP to neighboring buses, and where a significant number of elements are connected to the busbar. Based on this, we propose the following three metrics:

1) Metric ϕ – Sum of absolute LMP differences: This metric is defined as the sum of the absolute differences in LMPs $|\Delta_{LMP}|$ across all branches connected to the selected busbar. This metric rewards buses that have multiple, high Δ_{LMP} values and is inspired by congestion zone identification, Δ_{LMP} , and $\#$ of elements connected to the selected busbar metrics. If a busbar lies within a congestion zone, even if one of its branches exhibits a large Δ_{LMP} , the remaining connections are likely to have limited Δ_{LMP} values, thus limiting the value of BuS to reduce generation costs [43]. Moreover, the potential to find topological actions reducing the total costs increases with the number of elements connected to a busbar [25,26]. Thus, busbars exhibiting large Δ_{LMP} values over multiple incident branches are promising candidates.

2) Metric ξ – Number of congested branches: This metric evaluates the loading of the branches incident to a busbar and identifies the number of congested branches, inspired by a combination of the congestion zones identification and $\#$ of elements connected to the busbar metrics. A significant disparity in utilization of branches connected to the same busbar indicates the presence of local bottlenecks, where one or more branches operate closer to their thermal limits while others remain underutilized. Such imbalances suggest opportunities for remedial actions to redistribute flows, alleviate congestion, and therefore reduce generation costs by trying to use the cheapest generators to their maximum capacity.

3) Metric ζ – Binding voltage angle and magnitude limits: While a majority of existing work on OTS and BuS metrics has only considered DC-OPF representations, we base our metrics and optimization on AC-OPF (and approximations thereof) that also includes consideration of reactive power and voltage magnitudes. Specifically, the OPF includes voltage magnitude, voltage difference, and angle difference constraints for each branch. Branches with binding voltage magnitude or angle difference limits imply congestion and restricted power transfer capability. Identifying busbars connected by branches close to these operational limits highlights locations where topological actions can increase (or not) the grid transmission capacity.

TABLE III

Test cases from pglib [44] used in this work to test and validate the proposed metrics.

Test case	Name in pglib [44]	Generators	Buses	Branches	Loads
39-bus	case39_epri	10	39	46	21
118-bus	case118_ieee	54	118	186	99
793-bus	case793_goc	214	793	913	507
3374-bus	case3375wp_k	596	3374	4161	2434

B. Evaluation, testing and validation

To evaluate the metrics, we first solve an AC-OPF with the original topology to determine the generation costs. Then, we solve the LPAC-BuS model with one busbar selected for each run of the topology optimization model, and finally run an AC-OPF with the optimized topology as a feasibility check and to evaluate the cost reduction.

We use a testing phase where we leverage results from two small test systems to assess what combination of metrics effectively identifies the most relevant candidates for BuS. We first evaluate the results of enabling BuS for each busbar by computing both the metrics and the corresponding cost reduction for that busbar. Then, we leverage the results to find effective combinations of metrics. Since it is possible that we overfit our metrics to the specific test cases during the testing phase, we then implement a validation phase. In the validation phase, we apply the combination of metrics to two larger test cases and analyze their performance on this previously unseen data.

Table III lists the test cases from pglib [44] used in the testing and validation steps, including the number of generators, buses, branches, and loads in each test case. They range from 39 to 3374 buses.

C. Simulations setup

The results of the OPF and LPAC-BS models are computed using a MacBook Pro with chip M1 Max and 32 GB of memory, using Gurobi v12.0, MIP gap 0.01%, maximum simulation time for LPAC-BS, and Ipopt with linear solver ma97 for the OPF model.

IV. Results and discussion

A. Testing phase results

We perform the testing phase using the 39-bus and 188-bus test cases introduced in Table III.

1) Accuracy and Computational Efficiency: Using the 39-bus test case as an example, we first make some basic observations about the accuracy and computational effort associated with our approach. Fig. 2 plots the ϕ -metric of each busbar (representing the sum of absolute LMP differences across all the branches connected to the selected busbar) against the reduction in generation cost achieved by splitting that bus. Each busbar is represented by two dots, where the blue dot represents the results achieved with an LPAC-OPF feasibility check (FC) and the green dot represents the results achieved with the

AC-OPF FC. The FCs are run on the optimized topology computed through the LPAC-BuS model.

We observe that there are some differences between the two models, but that the trends (e.g. busbars with the highest ϕ values and the highest generation cost reductions) are similar. This shows that topology optimization through the LPAC-BuS model provides results that are sufficiently accurate to reduce the total costs of an AC-FC compared to the AC-OPF of the original topology. Therefore, the LPAC-BuS model computes topologies that are optimal and lead to a reduction in total costs compared to the original topology, even for AC-OPF formulations.

Regarding computational efficiency, the whole optimization process (splitting one busbar per time with LPAC-BuS, plus AC-FC and LPAC-FC) took 11.4 s, confirming the efficiency of the proposed LPAC-BuS model.

2) Testing of Metrics on 39-bus test case: From Fig. 2, we observe that BuS of buses 25, 3, 18, 26 and 4 lead to the biggest reductions in generation costs, while, interestingly, the two buses with highest ϕ -values, buses 30 and 2 do not reduce total costs.

Further analysis of the results yields some interesting insights. First, the branch connecting busbars 2 and 30 has the highest LMP difference Δ_{LMP} . However, when either of these buses is allowed to be split, the optimal topology is the same as the original one. Thus, there is no change in generation cost. This finding confirms that the widely used metric Δ_{LMP} is insufficient, and that we need more (or combined) metrics to select relevant busbars for topology optimization. Further, busbar 30 has only 2 elements connected to it, and its voltage magnitude U_{30}^m is at the upper limit 1.1. This suggests that it is important to also consider the # of elements connected to the selected busbar and the ζ -metric representing the presence of binding voltage angle and magnitude limits. Busbars 2 has 2 congested lines (used almost at full capacity) connected to it, confirming that the ξ -metric representing the number of congested lines might be important, but not when the busbar resides in a congested zone, as we commented in Section III-A.

3) 118-bus test case: We apply the previous findings to select busbars for splitting in the 118-bus case. Table IV shows the value of the different metrics as well as the cost reduction achieved with BuS for the buses with the highest ϕ -metric values (top) and busbars that lead to a cost decrease of $>0.05\%$, but are not in the top-10 ϕ -ranked busbars (bottom).

We observe that the busbars with high ϕ , many connected branches/elements and without binding voltage limits (ζ) lead to a cost decrease compared to the AC-OPF. Importantly, 4 out of 5 busbars with a cost reduction larger than 0.1% are included among the busbars with the highest ϕ values. The highest cost decrease is for busbar 69, whose optimized topology is shown in Fig. 3. In this optimized topology, power can directly flow from busbar 49 to 47, as the branches connecting them are decoupled from the original busbar 69.

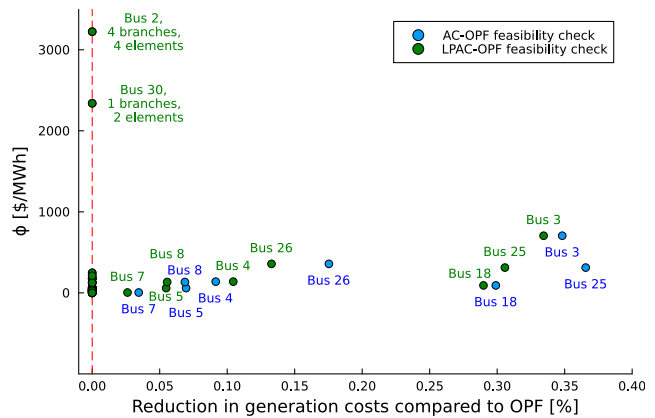


Fig. 2. For each bus in 39-bus test case, the optimal topology from the LPAC-BuS model is tested for an “AC”-OPF and “LPAC”-OPF feasibility check (FC). The differences in total costs of the FC compared to the original OPF are plotted on the x-axis, while the y-axis orders the busbar according to each bus’ sum of the absolute differences in LMPs over the branches connected to it (ϕ). The LPAC-FC and AC-FC see reductions in costs for the same buses.

TABLE IV

Metrics of the 10 busbars in the 118-bus test case with the highest sum of the absolute differences in LMPs over their branches (ϕ), and of the busbars with the highest cost decrease wrt AC-OPF, not in the top 10 ϕ -ranked busbars. Busbars at voltage limit (ζ) do not have a cost decrease, while there are limited congested ($> 85\%$ utilization) branches (ξ).

Busbar ID	ϕ [\$/MWh]	ϕ rank	# of branches	ξ [-]	# of elements	ζ [-]	% Cost decrease
69	2253.98	1	6	2	7	-	0.380
49	1836.24	2	12	1	14	-	0.344
100	1433.50	3	8	2	10	$U^{m,1.1}$	0.000
59	1168.27	4	7	0	9	-	0.156
47	827.49	5	3	1	4	-	0.000
66	665.04	6	5	0	7	$U^{m,1.1}$	0.000
103	570.94	7	4	1	6	-	0.039
56	559.88	8	6	0	8	-	0.017
65	552.91	9	4	0	5	-	0.000
77	509.41	10	7	0	9	-	0.132
80	371.05	19	8	0	10	-	0.143
42	326.99	22	4	0	6	-	0.098
44	115.77	57	2	0	3	-	0.097
45	192.69	41	3	0	4	-	0.091
43	206.29	37	2	0	3	-	0.064

Among the buses in the bottom part of Table IV, we observe that busbars 80 and 42 are connected to several branches. The other busbars decrease cost by not reconnecting branches to the split busbar, essentially performing transmission line switching rather than BuS. They are therefore more complex to identify with our metrics. Finally, all the busbars with a cost decrease of $>0.05\%$ are within the first half of the 118 ϕ -ranked busbars, and two of them have ϕ above its average value of 219.13 [\$/MWh].

Note that for this test case, the entire optimization process took 214.7 s. Based on these results, we consider busbars with several connected branches/elements and a ϕ above average as metrics to select relevant busbars in the validation step.

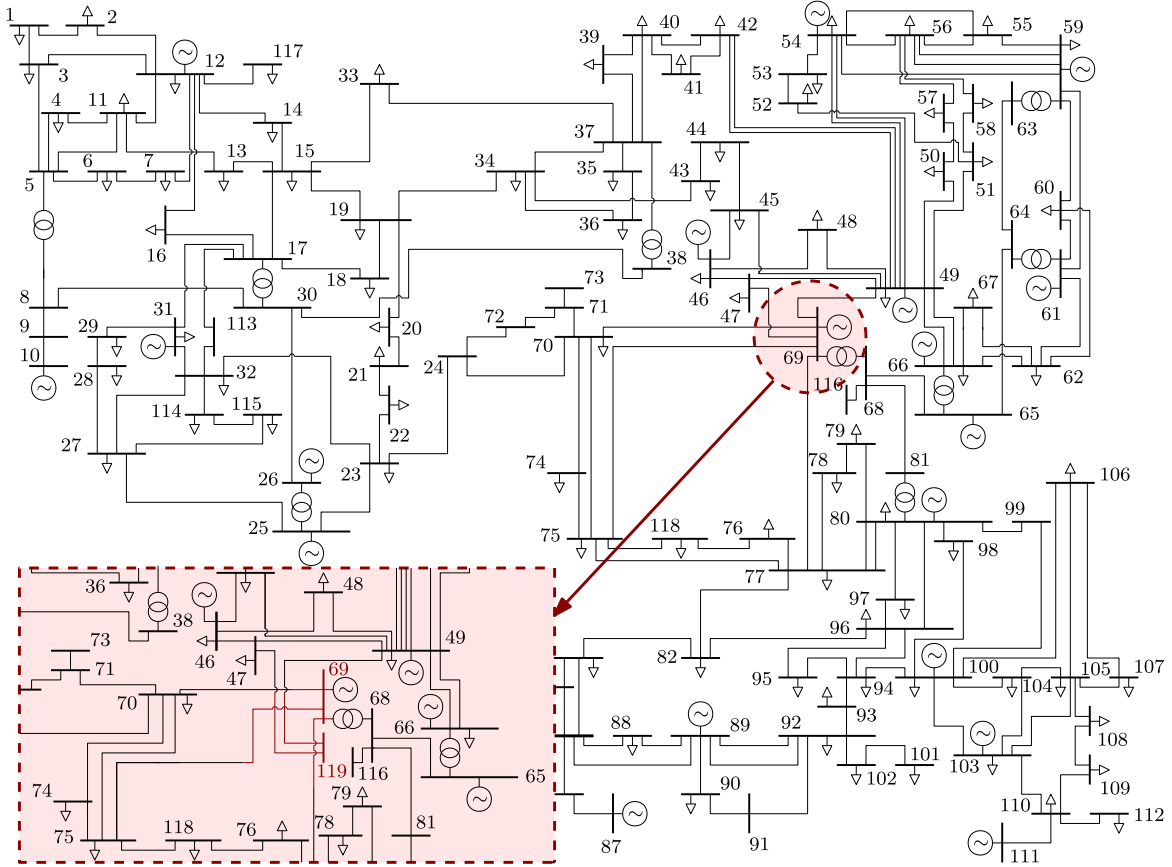


Fig. 3. Topology optimization model applied to busbar 69 in the 118-bus test case. In the optimized topology, busbars 47 and 49 are decoupled from busbar 69 and the neighboring busbars, leading to a reduction in the total generation costs of 0.380% compared to the original AC-OPF.

B. Validation phase results

In this step, we apply the metrics discussed above to identify busbars for splitting in the 793-bus and 3374-bus cases listed in Table III.

1) 793-bus test case: We first select the 15 busbars with the highest ϕ -values and remove those with fewer than 4 elements connected to them. As a result, the 8 busbars on the top part of Table V are selected. Second, we select the 7 busbars with the highest # of elements and branches connected to them, and have a ϕ higher than the mean ϕ value. These busbars are displayed on the bottom part of Table V. We ensure that all the selected busbars are connected to at most one congested line (ξ -metric ≤ 1) and have no binding voltage angle or magnitudes constraints (ζ -metric = 0).

The rightmost column of Table V shows the cost decrease for the identified busbars. As for the 118-bus case, selecting busbars with high ϕ values and larger # of connected branches/elements leads to cost decreases for several busbars, namely 693, 470, 649, 171 and 23. At the same time, the 7 busbars selected using the # of branches/elements and ϕ values above the mean- ϕ lead to cost reductions as well.

To validate whether we identified the “best” busbars for splitting, we validate our results by splitting every

TABLE V
Identification of 15 candidates for busbar splitting in the 793-bus test case with the proposed metrics, and related cost decrease. 12 optimized topologies out of 15 lead to a cost decrease in the AC-OPF.

Busbar ID	ϕ [\$/MWh]	ϕ rank	# of branches	ξ [-]	# of elements	% Cost decrease
693	2602.76	1	5	1	6	0.376
470	1630.23	2	3	1	4	0.650
406	1447.60	6	4	1	4	0.000
649	1230.62	9	4	0	5	0.274
677	1173.01	11	3	1	4	0.000
171	970.89	13	3	1	4	0.141
190	919.09	15	5	1	6	0.000
23	802.69	18	5	1	6	0.972
587	304.01	48	6	0	7	1.056
116	196.95	68	5	0	6	0.559
73	494.92	30	6	0	6	0.024
373	378.82	40	4	0	6	0.151
655	467.55	31	6	0	6	0.319
612	105.87	116	6	0	6	0.041
561	125.52	101	5	0	5	0.363

busbar in the system and checking the cost reduction. Fig. 4 shows the results obtained by splitting one busbar at a time for all busbars in the 793-bus system. We observe that the proposed metrics identify 3 of the 4 busbars that lead to the largest reductions in generation costs, as well as several other buses with high cost reductions. We note

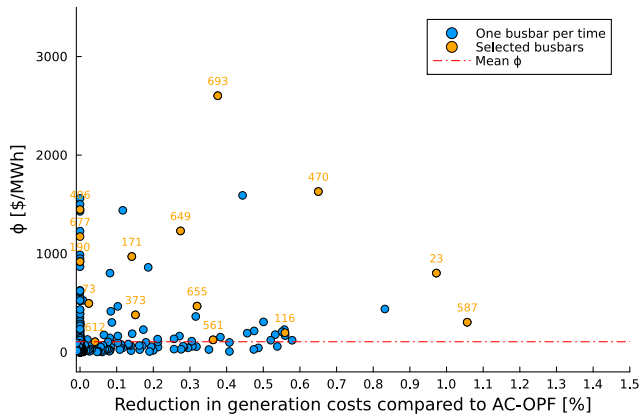


Fig. 4. Cost decrease of the AC-OPF feasibility check for the optimized topology of the selected busbars compared to the results obtained by splitting one busbar at a time for the 793-bus test case. Most of the busbars selected with the identified metrics do lead to a reduction in generation costs. The busbars with the highest cost decreases tend to have a sum of the absolute differences in LMPs across the branches connected to them (ϕ) higher than the mean ϕ value.

that busbar 444, which yields the third-best cost reduction if split, has only two connected branches, both of which are utilized above 80% of their rated capacity (one at 100%). As with most busbars in the bottom part of the previous Table IV, not reconnecting a branch to the split busbar is leading to 444's reduction in costs, suggesting that line switching rather than BuS is what achieves the cost reduction.

For this test case, splitting one busbar per time took 68102 s (19.14 h), 67639 s for the LPAC-BuS and 463.3 s for the AC-FC, while the total computational time to optimize only the the selected buses is considerably lower, with 3523.3 s (0.98 h).

2) 3374-bus test case: Finally, we use the same metrics as in the previous case to identify relevant candidates for BuS for the 3374-bus test case, too. On the top part of Table VI, the first 13 busbars are selected by considering the 20 busbars with the highest ϕ -values, and including the only ones with the highest ϕ and # of connected elements/branches. Note that busbars 679, 611 and 665 are selected even if they have a low number of branches, as their ϕ -values are high. In particular, busbars 679 and 611 have $\xi = 1$ and only two branches, as busbar 444 in the previous case, possibly leading to potential for line switching. The bottom part of Table VI shows 7 busbars selected based on their # of connected elements/branches and their above-average ϕ values. The mean ϕ value in this case is 483.55 [\$/MWh].

Table VI and Fig. 5 show that 8 of the selected busbar leads result in reductions in generation costs compared to the AC-OPF. Also in this case, part of the selected busbars, i.e., 498, 665, 439, and 670, are among those that lead to the largest cost decrease. Unlike case 793-bus, the busbars in the bottom part of Table VI do not lead to any cost reduction, even though they have several lines and elements connected to them. This result can be

TABLE VI
Identification of 20 candidates for busbar splitting in the 3374-bus test case with the proposed metrics, and related cost decrease.

Busbar ID	ϕ [\$/MWh]	ϕ rank	# of branches	ξ	# of elements	% Cost decrease
670	71334.40	1	5	1	10	0.048
671	57530.95	2	5	1	11	0.004
679	47530.03	3	2	1	3	0.000
611	36048.14	4	2	1	3	0.000
665	30099.63	5	3	0	4	0.079
254	26184.71	6	4	1	9	0.067
261	21423.57	7	5	1	6	0.000
441	18150.84	8	6	0	6	0.001
460	14854.40	11	4	0	4	0.072
499	14425.17	12	5	0	6	0.000
439	14047.40	13	7	0	8	0.063
498	11704.58	16	5	0	6	0.056
440	10713.17	18	5	0	5	0.000
10147	827.51	355	13	0	13	0.000
10153	901.66	320	13	0	13	0.000
10079	5648.17	43	12	2	10	0.000
10145	569.98	521	12	0	12	0.000
10063	486.84	602	12	0	12	0.000
10081	1463.67	191	12	0	11	0.000
10158	543.18	544	12	0	12	0.000

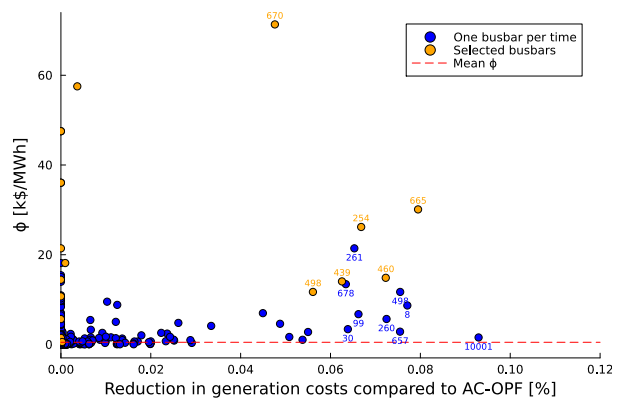


Fig. 5. Cost decrease of the AC-OPF feasibility check for the optimized topology of the selected busbars compared to the results obtained by splitting one busbar at a time for the 3374-bus test case. The proposed metrics identify several busbars leading to the highest reductions in generation costs.

attributed to the lower cost reductions relative to previous test cases, indicating that large cost reductions are not achievable in this specific test case, and that identifying relevant busbars for BuS is therefore more challenging. For example, busbar 10001 yields the largest cost reduction, even though it has 4 non-congested branches connected to it and a low ϕ , making it difficult to identify as a good candidate from the OPF results. In addition, out of the busbars with high ϕ -values and low number of branches (679, 611 and 665), only 665 leads to a cost decrease if split. We leave further refinements of the metrics to efficiently select busbars with similar characteristics for future work. Nevertheless, Fig. 5 still confirms the validity of the proposed metrics in identifying relevant busbars for BuS, with several selected busbars being among the ones leading to the highest cost reductions compared to the AC-OPF simulation.

Finally, optimizing the selected buses took 13582.7 s (3.77 h), or an average of 11.32 min per bus. Therefore, the proposed metrics select relevant busbars substantially faster than splitting one busbar at a time, which took 374.98 h (15.62 days).

V. Conclusion and future work

This paper identifies relevant metrics to determine the best busbar candidates for busbar splitting based on the results of optimal power flow simulations. We propose new metrics and combine them with existing ones in the literature. Through a testing step to refine the metrics and a validation step, we show that the proposed metrics effectively identify busbars whose optimized topology leads to lower generation costs compared to an AC-OPF simulation.

Specifically, the results show that our newly proposed ϕ -metric, defined as the sum of the absolute differences in LMPs over the branches connected to a busbar (ϕ), in combination with the $\#$ of elements connected to the busbar, can help identify the busbars that achieve the highest cost reductions. Further, the presence of binding voltage angle and magnitude limits (ζ -metric) indicates that busbar splitting will likely not reduce cost. Some of the buses that were not identified by our metrics achieved cost reductions through transmission line switching rather than busbar splitting.

Given the flexibility of the proposed grid topology optimization model in including more than one busbar, future work will include testing combinations of busbars to achieve further reductions in generation costs. Moreover, the proposed metrics can be used in grid planning side to investigate the possibility of retrofitting existing substations to effective topological actions when congestion takes place in the grid, or new substations or RES capacity are installed in the grid.

Acknowledgement

This work is supported by the Belgian Energy Transition Fund, FOD Economie, project DIRECTIONS, and a Research Foundation – Flanders (FWO) travel grant for Giacomo Bastianel’s research visit to UW-Madison.

References

- [1] International Energy Agency, “Electricity grids and secure energy transitions.” [Online] Available: <https://www.iea.org/reports/electricity-grids-and-secure-energy-transitions>. (accessed July 3, 2025), 2023.
- [2] IRENA, “World Energy Transitions Outlook 2023.” [Online] Available: <https://www.irena.org>. (accessed July 3, 2025), 2023.
- [3] ACER, “Transmission capacities for cross-zonal trade of electricity and congestion management in the EU.” [Online] Available: <https://www.acer.europa.eu>. (accessed July 6, 2025), 2025.
- [4] N. Shreve, J. Selker, Z. Zimmerman, and R. Gramlich, “2023 transmission congestion report.” [Online] Available: https://gridstrategiesllc.com/wp-content/uploads/Grid-Strategies_2023-Transmission-Congestion-Report.pdf (accessed July 6, 2025), 2024.

- [5] N. Shreve, J. Selker, Z. Zimmerman, and R. Doying, “Transmission congestion for 2024.” [Online] Available: https://gridstrategiesllc.com/wp-content/uploads/GS_Transmission-Congestion-for-2024.pdf (accessed February 11, 2026), 2025.
- [6] SMARD.de, “Congestion management.” [Online] Available: <https://www.smard.de/page/en/topic-article/5790/214060/congestion-management> (accessed July 6, 2025), 2025.
- [7] European Commission, JRC, “Redispatch and congestion management.” [Online] Available: <https://data.europa.eu/doi/10.2760/853898>, JRC137685. (accessed July 3, 2025), 2024.
- [8] International Energy Agency, “The clean energy economy demands massive integration investments now.” [Online] Available: <https://www.iea.org/commentaries>. (accessed August 14, 2025), 2024.
- [9] International Energy Agency, “Building the future transmission grid - strategies to navigate supply chain challenges.” [Online] Available: <https://www.iea.org>. (accessed August 21, 2025), 2025.
- [10] M. Neukirch, “Grinding the grid: Contextualizing protest networks against energy transmission projects in southern germany,” *Energy Research & Social Science*, vol. 69, p. 101585, 2020.
- [11] O. Mirzapour, X. Rui, and M. Sahraei-Ardakani, “Grid-enhancing technologies: Progress, challenges, and future research directions,” *Electric Power Systems Research*, vol. 230, p. 110304, 2024.
- [12] EPRI, “Transmission Topology Optimization, State-of-the-Art White Paper: A GET SET White Paper.” [Online] Available: <https://www.epri.com/research> (accessed July 6, 2025), 2025.
- [13] CCR Core TSO Cooperation, “Explanatory document to the Core Capacity Calculation Region methodology for common provisions for regional operational security coordination in accordance with Article 76 of Commission Regulation (EU) 2017/1485.” [Online] Available: <https://acer.europa.eu/sites/default/files/documents/en/Electricity>. (accessed March 6, 2026), 2019.
- [14] WATT coalition, “Congestion & overload mitigation with transmission reconfigurations.” [Online] Available: <https://www.brattle.com/insights-events/publications/congestion-overload-mitigation-with-transmission-reconfigurations-experience-in-miso-and-spp/> (accessed March 6, 2026), 2022.
- [15] R. Bacher and H. Glavitsch, “Network topology optimization with security constraints,” *IEEE Transactions on Power Systems*, vol. 1, no. 4, 1986.
- [16] E. B. Fisher, R. P. O’Neill, and M. C. Ferris, “Optimal transmission switching,” *IEEE Transactions on Power Systems*, vol. 23, no. 3, 2008.
- [17] K. W. Hedman, R. P. O’Neill, E. B. Fisher, and S. S. Oren, “Optimal transmission switching with contingency analysis,” *IEEE Transactions on Power Systems*, vol. 24, no. 3, pp. 1577–1586, 2009.
- [18] M. Heidarifar, M. Doostizadeh, and H. Ghasemi, “Optimal transmission reconfiguration through line switching and bus splitting,” in *IEEE PES General Meeting*, pp. 1–5, 2014.
- [19] A. A. Mazi, B. F. Wollenberg, and M. H. Hesse, “Corrective control of power system flows by line and bus-bar switching,” *IEEE Transactions on Power Systems*, vol. 1, no. 3, pp. 258–264, 1986.
- [20] E. Makram, K. Thornton, and H. Brown, “Selection of lines to be switched to eliminate overloaded lines using a z-matrix method,” *IEEE Transactions on Power Systems*, vol. 4, no. 2, pp. 653–661, 1989.
- [21] K. W. Hedman, S. S. Oren, and R. P. O’Neill, “A review of transmission switching and network topology optimization,” in *2011 IEEE PES General Meeting*, pp. 1–7, 2011.
- [22] K. W. Hedman, R. P. O’Neill, E. B. Fisher, and S. S. Oren, “Optimal transmission switching—sensitivity analysis and extensions,” *IEEE Transactions on Power Systems*, vol. 23, no. 3, pp. 1469–1479, 2008.
- [23] M. Heidarifar and H. Ghasemi, “A network topology optimization model based on substation and node-breaker modeling,” *IEEE Transactions on Power Systems*, vol. 31, no. 1, pp. 247–255, 2016.

- [24] A. Hinneck, B. Morsy, D. Pozo, and J. Bialek, "Optimal Power Flow with Substation Reconfiguration," in *IEEE PowerTech*, pp. 1–6, 2021.
- [25] M. Heidarifar, P. Andrianesis, P. Ruiz, M. C. Caramanis, and I. C. Paschalidis, "An optimal transmission line switching and bus splitting heuristic incorporating AC and N-1 contingency constraints," *International Journal of Electrical Power & Energy Systems*, vol. 133, p. 107278, 2021.
- [26] B. Morsy, A. Hinneck, D. Pozo, and J. Bialek, "Security constrained OPF utilizing substation reconfiguration and busbar splitting," *Electric Power Systems Research*, vol. 212, p. 108507, Nov. 2022.
- [27] G. Bastianel, M. Vanin, D. Van Hertem, and H. Ergun, "Optimal Transmission Switching and Busbar Splitting in Hybrid AC/DC Grids," arXiv:2412.00270, 2024.
- [28] B. Morsy, M. Deakin, A. Anta, and J. Cremer, "Corrective soft bus-bar splitting for reliable operation of hybrid AC/DC grids," *International Journal of Electrical Power & Energy Systems*, vol. 169, p. 110792, 2025.
- [29] G. Bastianel, D. Van Hertem, H. Ergun, and L. Roald, "Day-ahead transmission grid topology optimization considering renewable energy sources' uncertainty," *International Journal of Electrical Power & Energy Systems*, vol. 174, p. 111527, 2026.
- [30] M. Van Deyck, G. Bastianel, G. Chaffey, H. Ergun, and D. Van Hertem, "Techno-economic comparison of preventive DC-side decoupling and DC circuit breakers in multiterminal offshore HVDC grids," *IET Conference Proceedings*, vol. 2025, pp. 137–144, 2025.
- [31] S. Mohammad, Y. Hatim, and L. Zuyi, *Market Operations in Electric Power Systems: Forecasting, Scheduling, and Risk Management*. Wiley-IEEE, 2002.
- [32] D. Kirschen and G. Strbac, *Fundamentals of power system economics*. Wiley, 2004.
- [33] P. A. Ruiz, J. M. Foster, A. Rudkevich, and M. C. Caramanis, "On fast transmission topology control heuristics," in *2011 IEEE PES General Meeting*, pp. 1–8, 2011.
- [34] J. D. Fuller, R. Ramasra, and A. Cha, "Fast heuristics for transmission-line switching," *IEEE Transactions on Power Systems*, vol. 27, no. 3, 2012.
- [35] P. A. Ruiz, J. M. Foster, A. Rudkevich, and M. C. Caramanis, "Tractable transmission topology control using sensitivity analysis," *IEEE Transactions on Power Systems*, vol. 27, no. 3, pp. 1550–1559, 2012.
- [36] M. Khanabadi, H. Ghasemi, and M. Doostizadeh, "Optimal transmission switching considering voltage security and n-1 contingency analysis," *IEEE Transactions on Power Systems*, vol. 28, no. 1, pp. 542–550, 2013.
- [37] Y. Zhou, A. S. Zamzam, A. Bernstein, and H. Zhu, "Substation-level grid topology optimization using bus splitting," in *ACC Conference*, 2021.
- [38] L. Wang and H.-D. Chiang, "Bus-bar splitting for enhancing voltage stability under contingencies," *Sustainable Energy, Grids and Networks*, vol. 34, p. 101010, 2023.
- [39] S. Babaeinejadsarookolae, B. Lesieutre, and C. L. DeMarco, "Tractable iterative transmission topology control heuristics based on node-breaker modeling," in *UPEC Conference*, 2021.
- [40] ENTSO-e, "Grid incident in Spain and Portugal on 28 April 2025." [Online] Available: https://www.entsoe.eu/publications/blackout/28-april-2025-iberian-blackout/Publications_&_Documents (accessed March 6, 2026), 2025.
- [41] C. Coffrin, R. Bent, K. Sundar, Y. Ng, and M. Lubin, "Powermodels.jl: An open-source framework for exploring power flow formulations," in *PSCC*, pp. 1–8, June 2018.
- [42] C. Coffrin and P. Van Hentenryck, "A linear-programming approximation of ac power flows." <https://arxiv.org/abs/1206.3614>, 2013.
- [43] C. Coffrin, H. L. Hijazi, K. Lehmann, and P. Van Hentenryck, "Primal and dual bounds for optimal transmission switching," in *2014 PSCC*, pp. 1–8, 2014.
- [44] S. Babaeinejadsarookolae and et al., "The Power Grid Library for Benchmarking AC Optimal Power Flow Algorithms." <https://arxiv.org/abs/1908.02788>, 2021.